

## Raman line asymmetry in alloys and in ion-implanted polar crystals

O. Brafman and R. Manor

*Department of Physics and Solid State Institute, Technion-Israel Institute of Technology, 32000 Haifa, Israel*

(Received 26 July 1994)

We compare the effect of ion bombardment with that of alloying on the Raman-scattering line shape and its phonon frequency. In the case of ion implantation (no annealing), the modifications are attributed to the confinement dictated by the spatial correlation of the phonons and the formation of disorder therein, which partially relaxes the selection rules causing a clear dependence on the dispersion relations. We present results taken on GaAs, InP, and  $\text{Al}_x\text{Ga}_{1-x}\text{As}$ , for both TO and LO lines. Our results agree with the main assumptions of the spatial-correlation model and add information about the phonon-dispersion relations. As opposed to that, the asymmetry of the Raman line shape of  $\text{Al}_x\text{Ga}_{1-x}\text{As}$  alloys is explained here in a totally different way. It is assumed that the random cation distribution (with no clustering) gives rise to a collection of various phonon modes having the same symmetry, which, therefore, interact with each other. This interaction transfers charge, such that in the case of LO modes the more ionic LO mode is favored, while in the case of TO modes the mode favored is the one of the stronger bond. This implies that in both cases the mode exhibiting the higher frequency strengthens, causing asymmetry. The alloy disorder-activated modes under resonance conditions are also discussed.

### I. INTRODUCTION

The crystalline order in semiconductors is evidently of major importance for both technology and basic research. This is the motivation for the large variety of experimental methods that have been applied to attain a model suited to describe the effects of the disorder and attempt to make it quantitative. This has been the subject of many reports during the last two decades.

We shall restrict our study to two mechanisms that generate crystallographic disorder (mainly in III-V compounds): that arising by ion implantation<sup>1-4</sup> (no annealing) and that formed by alloying.<sup>5-7</sup> Reference is made in these alloys to two-mode behavior of the phonon optic branches, for which at each intermediate concentration, two reststrahlen bands exist. The Raman line shapes will be used to study the disorder in the samples. The phonon lines observed in the Raman spectra of both ion-bombarded and alloyed samples show a substantial asymmetry; this is particularly striking in the case of LO phonon lines, but occurs also in TO lines, which were overlooked in the past.

An attempt was made to attribute the phonon line asymmetry of both these two distinct systems to the phonon-dispersion relation through a single model, that of spatial correlation.<sup>1,5</sup> This model<sup>1,8</sup> assumes that the generation of disorder restricts the phonon correlation length, and this finite-size effect causes a violation of selection rules, which allows for weighted contributions to Raman scattering from the entire Brillouin zone (BZ). The application of this model to the case of alloys was challenged by Kash *et al.*,<sup>9</sup> arguing that a well-defined  $\mathbf{k}$  is present in this case. A similar conclusion was reached earlier by McGlenn *et al.*<sup>10</sup> As for the ion-implanted system, we have not found in the literature an unambiguous contradiction to this attitude.

Our aim is to examine the possible mechanisms that

are responsible for the asymmetry of the Raman lines in these two systems and to point out the dissimilarity between the sources for which these arise. It was pointed out by Zallen<sup>11</sup> that compositional disorder (as is the case in alloys) is mild compared to the topological disorder characteristic of amorphous solids (as is approached by ion bombardment), because there is an underlying crystal lattice with its periodicity preserved. The asymmetry of the Raman lines in alloys was earlier attributed to anharmonicity<sup>12</sup> due to phonon-phonon interaction or to Fano-type interaction<sup>13</sup> of a single phonon mode with a continuous spectrum of excitations having the same symmetry. In the phonon-dispersion calculation using large supercells by Baroni, de Gironcoli, and Giannozzi<sup>14</sup> this asymmetry was reproduced.

We shall support the spatial-correlation model as related to ion implantation with one restriction; we shall only refer to a correlation length within which the phonon exists. We shall therefore use the term crystallite in the sense of the volume having the average dimensions of the correlation length. Such crystallites may be formed due to nonhomogeneity of the damage the ion bombardment produces. We shall offer a different explanation for the asymmetry of the Raman phonon lines in alloys. This does not exclude other possible mechanisms, but rather calls attention to what we consider a major factor in all alloys and also indicates a measure for the effect. Finally, in the context of the present study we also discuss the disorder-activated modes which appear in alloys at resonance conditions.

### II. EXPERIMENT

The samples examined were GaAs, InP, and  $\text{Al}_x\text{Ga}_{1-x}\text{As}$  with  $x=0.3$ ,  $0.7$ , and  $0.85$ . The  $\text{Al}_{0.70}\text{Ga}_{0.30}\text{As}$  samples were grown by both molecular-beam epitaxy (MBE) and metal-organic chemical-vapor

deposition (MOCVD) and the  $\text{Al}_{0.30}\text{Ga}_{0.70}\text{As}$  and  $\text{Al}_{0.85}\text{Ga}_{0.15}\text{As}$  samples were grown by MOCVD, all in the [001] direction. The thickness of the  $\text{Al}_x\text{Ga}_{1-x}\text{As}$  layer was about  $0.8\ \mu\text{m}$  (for  $x=0.7$ ) and  $0.5\ \mu\text{m}$  (for  $x=0.3$  and  $0.85$ ) to allow for studying the (110) cleaved plane. The  $\text{Al}_{0.70}\text{Ga}_{0.30}\text{As}$  and  $\text{Al}_{0.85}\text{Ga}_{0.15}\text{As}$  samples were capped by a  $50\text{-\AA}$ -thick layer of GaAs. In all the samples the free-carrier density was of the order of  $10^{16}\ \text{cm}^{-3}$  or less. Ions of  $\text{B}^+$  were implanted at 50 keV with fluences between  $1 \times 10^{13}$  and  $1 \times 10^{15}$  ion  $\text{cm}^{-2}$  with no subsequent annealing; moreover, the implantation current was kept low enough to avoid annealing during the process. The implantation was directed at a small angle to the [001] or the [110] directions. In each case a mask was used such that implanted and nonimplanted regions were examined on the same sample.

The room-temperature micro-Raman spectra were excited mainly by  $\text{Ar}^+$  laser lines, keeping the power low in order to prevent heating and free-carrier excitation. The 1.96 eV excitation energy of a He-Ne laser was also used to examine the effect of lower-than-gap excitation. These spectra were analyzed by a Dilor Triplemate spectrometer with 1800 grooves/mm gratings and equipped with a cooled charge-coupled device detector. The spectra, both polarized and depolarized, were taken using  $\times 100$  magnification at a backscattering configuration from the (001) and (110) planes. We use  $\mathbf{x} \equiv [100]$  and  $\mathbf{x}' \equiv [110]$ .

### III. RESULTS AND DISCUSSION

We start with the effect of ion implantation, showing that the phonon dispersion has a major role in the reshaping of the Raman lines and in the shifting of their frequencies as a result of the ion bombardment. One should take note of the fact that in Raman scattering the laser wavelength probe is of the order of  $0.5\ \mu\text{m}$ ; this is therefore the order of the phonon wavelength (when the correlation length is larger) and it allows for the observation of phonons in the presence of the considerable damage caused by the implantation of the light ions used. However, it is true that in addition to the damaged crystallites, "pure" amorphous regions do also develop, which also show up in the Raman spectra. We therefore should consider a mixture of these two phases, the phonons of which do not intermix.<sup>11</sup> It is not strictly a two-mode behavior, as there is no interaction between the two phases, because these are separated spatially. Moreover, the phonons of the amorphous regions are not affected by the neighboring crystallites (these phonons reflect the density of states, allowing all  $\mathbf{k}$  values). Also the crystallites are not affected by the neighboring amorphous regions except for the additional confinement imposed by those regions. The increase of the implanted dose enhances the amorphous volume, reduces the crystallites' size, and thereby emphasizes the phenomena related to the quantum size effects. In order to study the surviving crystallite net effect, the amorphous contribution has to be subtracted from the Raman spectrum. Strictly speaking, this cannot be done because of the partial selection-rule breaking of the crystallites. Nevertheless, a reasonable approximation is obtained when the Raman spec-

trum taken from an amorphous sample at the same polarization configuration is factorized to cancel the amorphous contribution in the partially amorphized sample at a spectral region away from that of the studied phonons of the crystallites. Along with the allowed studied mode (either TO or LO) a weak line of the other mode (either LO or TO) is also present. By subtracting the respective forbidden spectrum with a suitable (low) weight, the amorphous adjustment is taken care of and the actual line shape is recovered. The main features, the asymmetry and the frequency shift, still persist, though in a more moderate fashion. We assume that the regions responsible for that are therefore not necessarily as small as concluded earlier. Moreover, in each crystallite of size  $L$ , phonons are created with predominantly  $k = 2\pi/L$  and the corresponding frequencies are imposed by the phonon-dispersion relations. The distribution in the size of the crystallites should be reflected in the line shape if that were the only effect. In addition, account should be taken of the degree of damage that each such crystallite suffers by the ion implantation, which is pronounced in terms of the increase in the Raman linewidth and the violation of the selection rules. We thus would have liked to separate the confinement that results from the finite-size effect of the crystallite and the disorder therein, but these are two inseparable effects. Within the ion-bombardment process, at the first stages the disorder is the main effect and the infinite-correlation characteristic of a single crystal may still hold. Only at later stages with heavier bombardment these two effects are formed simultaneously. In fact, with growing ion fluence the LO line widens at first with no shift and only at a high enough dose the broadening is accompanied by a frequency shift.<sup>4</sup>

Our experiments related to ion bombardment were performed on three different systems, each at the backscattering configuration, both parallel to the [001] and the [110] directions, displaying either the LO or the TO lines, respectively. The three systems studied by ion implantation were GaAs, for which the dispersion of both TO and LO modes is negative [the frequency decreases with increasing  $\mathbf{k}$ ,  $(\partial\omega/\partial k) < 0$ ]; InP, where the LO dispersion is rather small but negative and that of the TO mode is positive;<sup>15</sup> and  $\text{Al}_x\text{Ga}_{1-x}\text{As}$ , where the dispersion of the AlAs-like LO mode ( $\text{LO}_2$ ) was calculated<sup>14</sup> to be negative but small compared with the corresponding GaAs-like mode ( $\text{LO}_1$ ). The calculation of the AlAs-like TO branch ( $\text{TO}_2$ ) yields a negative dispersion similar to that of the GaAs branch ( $\text{TO}_1$ ) and even somewhat larger. This has also been verified experimentally via Raman scattering from GaAs-AlAs superlattices.<sup>16,17</sup> While the neutron-scattering data of GaAs are reliable and are backed by a well-fitted calculated phonon dispersion, those of the optic branches of InP show a significant experimental uncertainty,<sup>15</sup> and we have not found a supportive calculation. In the case of AlAs no neutron-scattering data are available. We shall now discuss each of these samples separately.

Figure 1 demonstrates the effect of  $10^{14}$  ion  $\text{cm}^{-2}$   $\text{B}^+$  implantation on the LO and TO modes of GaAs in the respective allowed configurations [ $z(yx)\bar{z}$  and  $x'(y'z)\bar{x}'$ ].

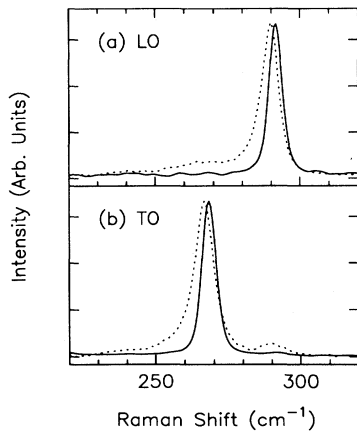


FIG. 1. Raman scattering from LO (a) and TO (b) phonons of GaAs (solid line) and after ion implantation (dotted line). Excitation energy 2.41 eV.

The implantation obviously enhances the forbidden part of the spectra, along with the disorder-induced structure. The additional most important features are the frequency downshift, the line broadening, and an asymmetry tail developed at the low-frequency side of each line, which is about the same for both of them within the experimental accuracy. This agrees qualitatively with the negative slope of the dispersion of the two phonon branches.<sup>18</sup> Also, the line peak frequencies have shown the same downshift with the implantation fluence. Inspecting more carefully the phonon dispersion, a similar slope is found for both branches at reasonable wave vectors (say,  $\frac{1}{5}$  of the BZ), which suggests that for that implantation dose the main contribution comes primarily from the low-wave-vector zone, while the contributions from larger  $k$  are of significantly lower weight; altogether the frequency difference between the  $\Gamma$  and the  $X$  points for the LO branch is almost twice that of the TO branch.<sup>18</sup>

Figure 2 shows the LO and TO Raman lines of pristine

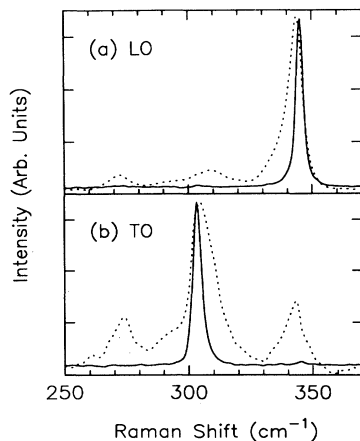


FIG. 2. Raman scattering from LO (a) and TO (b) phonons of InP (solid line) and after ion implantation (dotted line). Excitation energy 2.41 eV.

InP compared with those of  $B^+$ -implanted InP at a dose of  $10^{14}$  ion  $cm^{-2}$ . The same ion flux produces a larger crystallographic disorder in InP, as is reflected by the intense forbidden parts of the spectra and the appearance of extra lines, especially that at  $272$   $cm^{-1}$ , which has also been seen elsewhere, but was incorrectly assigned.<sup>19</sup> In the InP spectrum the LO line is slightly asymmetrical and its frequency is downshifted. As opposed to that, the TO line frequency is *upshifted* and exhibits a larger asymmetry, but towards the high-frequency side. This in itself shows a tight link to the dispersion of the optic branches. When more carefully examined, it is found that the forbidden LO line is lower in frequency with regard to that of the allowed LO mode [Fig. 2(a)], while the opposite is true with regard to the allowed and forbidden TO modes; there the difference is even more pronounced. All these observations qualitatively confirm the dispersion obtained by neutron scattering.<sup>15</sup> The basic difference between the two implanted systems shows that the phonon dispersion has a major role in shaping the Raman lines and shifting their frequencies under implantation. But this does not mean that it is the only cause.

This conclusion is further supported by the behavior of the third system,  $Al_{0.70}Ga_{0.30}As$ , under an implantation dose of  $5 \times 10^{14}$  ion  $cm^{-2}$ , shown in Fig. 3 for the AlAs-like mode. Here, the  $LO_2$  line only slightly downshifts with the implanted dose, while the  $LO_1$  line downshifts considerably more for the same implanted dose, nearly as much as the LO line of the GaAs capping. This follows nicely the calculated small negative dispersion of the AlAs branch,<sup>14</sup> though it suggests a larger negative dispersion of the GaAs branch than that calculated for the concentration examined here. We deliberately ignored the LO line shape of these two lines in the nonimplanted region. The effect of the ion implantation on the  $TO_2$  mode is even more impressive; both its frequency downshift and the asymmetry are larger than those of the  $LO_2$  line for the same dose, which is in line with the calculated dispersion.<sup>14</sup> Therefore, in all three systems, the frequency shift and the line shape as the result of ion

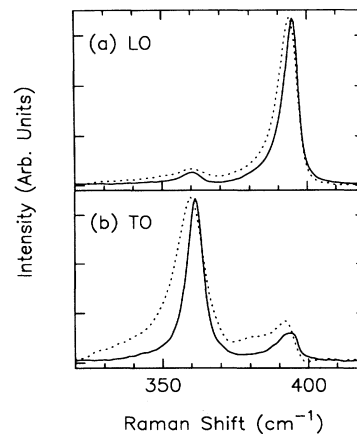


FIG. 3. Raman scattering from  $LO_2$  (a) and  $TO_2$  (b) phonons of  $Al_{0.70}Ga_{0.30}As$  (solid line) and after ion implantation (dotted line). Excitation energy 2.41 eV.

bombardment follow the phonon-dispersion relation as is primarily assumed by the spatial-correlation model. The results reported on implanted GaP imply similar conclusions.<sup>4</sup> The flat TO branch causes a small frequency shift and a small asymmetry, very much smaller than in the respective steep LO branch.

We now move on to the phonon Raman line shape of the optic modes of two-mode-type alloys. Practically all III-V alloys show two-mode behavior. There is *no* justification for using the spatial-correlation model in such a system,<sup>5</sup> because in a well-controlled crystal growth the correlation length should be considered infinite, unless massive clustering is present. This means that we agree with the conclusion<sup>9,10</sup> that  $\mathbf{k}$  is fairly well defined in alloys. However, there is obviously an asymmetry in the LO lines and often a smaller asymmetry in the TO lines when it occurs, and it ought to be explained. The asymmetry is particularly manifested in the case of LO<sub>2</sub> modes, whether it is in Al<sub>x</sub>Ga<sub>1-x</sub>As (Ref. 12) or in Al<sub>x</sub>In<sub>1-x</sub>As.<sup>20</sup> There is a substantial contradiction between the calculated flat LO<sub>2</sub> dispersion and its extensive asymmetry, especially in that the line asymmetry is far more pronounced in the LO<sub>2</sub> mode compared to LO<sub>1</sub> for both Al<sub>0.70</sub>Ga<sub>0.30</sub>As and Al<sub>0.30</sub>Ga<sub>0.70</sub>As. If one tries to account for the asymmetry by applying the spatial-correlation model, one has to assume the participation of phonons from the entire BZ, and even this will not lead to a reasonable fit if that flat LO<sub>2</sub> branch verified earlier is considered. The same is true in the case of Al<sub>x</sub>In<sub>1-x</sub>As and even more so in the AlAs-like modes of the quaternaries containing AlAs.<sup>20</sup> But the flatness of the calculated LO<sub>2</sub> branch<sup>14</sup> rules out the interpretation of the asymmetry in terms of the spatial-correlation model. The TO<sub>2</sub> branch is calculated<sup>14</sup> to have a negative dispersion, larger than that of the LO<sub>2</sub>, but as can be seen in Fig. 3(b) the TO<sub>2</sub> line is nearly symmetrical. This implies at the most only a minor effect of the phonon dispersion on the phonon line shape in the case of alloys.

In examining *all* the mixed-crystal systems it is found that in two-mode-type systems, while the TO frequency may shift either way with mixing, the LO line frequency is *always* reduced with the dilution of the component of the alloy responsible for the mode under consideration. The LO and TO branches generally emerge at the local-(gap-) mode frequency, which is triply degenerate.<sup>21</sup> The reduction in the LO frequency is caused by the drop in the macroscopic electric field associated with that mode; this is a result of the decrease in the dipole density as well as the lowering of the ionicity with alloying. The frequency change of the TO lines reflects the change in the bonding. In the case of two interacting oscillators of the same nature (having the same symmetry), either that of higher ionicity or that of the stronger bond gains in oscillator strength at the expense of the other mode<sup>22,23</sup> and therefore its intensity is enhanced. With this in mind we shall now examine the behavior of LO and TO modes in alloys, starting with the LO mode. We shall restrict the present discussion to Al<sub>x</sub>Ga<sub>1-x</sub>As, where the frequency distance between the GaAs and the AlAs oscillators is large enough that the coupling between them can be neglected. We can therefore deal with the GaAs-like os-

illator and the AlAs-like oscillator as independent entities.

The nature of the phononic oscillators in alloys is somewhat confusing. Verleur and Barker<sup>24</sup> proposed an analysis based on five different building blocks of the tetrahedral structure with As at the center and either Ga or Al at the corners of the tetrahedron. When clustering is left out, these blocks are assumed to be randomly distributed in accordance with the given concentration. This leads to a broadening of the Raman line as well as an asymmetry changing sign, which would be concentration dependent. That is not found experimentally, but we shall nevertheless adapt this overall model, slightly modified. We shall consider a buildup of modes arising from the different building blocks, but, since these modes exhibit the same symmetry and are close in frequency, we assume an interaction (interference) among these modes. We believe that this is built into the calculation which reproduces the asymmetry, using a large supercell.<sup>14</sup> This interaction transfers oscillator strength from the less to the more ioniclike mode<sup>22</sup> (dealing with the LO modes first) and repels them apart. This interaction will then cause the LO line to be asymmetric by increasing the weight of the intensity of the higher-ionicity modes, which corresponds to the higher-frequency modes. This should be true for *all* alloys, but is expected to be more pronounced for LO lines, for which the slope of the frequency with the concentration,  $\partial\omega/\partial x$ , is larger. This is the case for the AlAs-like LO mode in Al<sub>x</sub>Ga<sub>1-x</sub>As (Ref. 12) and in Al<sub>x</sub>In<sub>1-x</sub>As (Ref. 20) and also in II-VI alloys such as ZnS<sub>x</sub>Se<sub>1-x</sub>.<sup>25</sup>

As for the TO lines, the mechanism that governs the transfer of strength is that of the bond variation with concentration;<sup>22</sup> the shorter the bond, the higher the frequency, and the larger the intensity. Therefore asymmetry is also found in TO lines, depending on the slope of the frequency vs concentration. The frequency of the TO<sub>2</sub> line in Al<sub>x</sub>Ga<sub>1-x</sub>As changes by only 3 cm<sup>-1</sup> for the full range of  $x$  and indeed the TO line is nearly symmetric [see Fig. 3(b) and Table I]. Moreover, such a sample, when being ion implanted, develops a considerable asymmetry of that TO line. Again, this verifies that, while the line shape modified by ion bombardment is dispersion dependent,

TABLE I. Frequency shift caused by implantation ( $\Delta\omega = \omega_{\text{imp}} - \omega_0$ ).  $P_0$  and  $P_{\text{imp}}$  are the line asymmetry (width ratio of the low- to high-frequency component at half maximum) of pristine and implanted samples. The doses are  $1 \times 10^{14}$  ion cm<sup>-2</sup> for GaAs and InP and  $5 \times 10^{14}$  ion cm<sup>-2</sup> for Al<sub>0.70</sub>Ga<sub>0.30</sub>As.

Sample	Mode	$\Delta\omega$ (cm <sup>-1</sup> ) ±0.3	$P_0$ ±0.10	$P_{\text{imp}}$ ±0.10
GaAs	LO	-1.8	1.00	1.19
	TO	-1.6	1.00	1.18
InP	LO	-1.7	1.07	1.23
	TO	+1.2	0.89	0.61
Al <sub>0.70</sub> Ga <sub>0.30</sub> As	LO <sub>2</sub>	-1.0	1.42	1.44
	TO <sub>2</sub>	-1.8	1.15	1.27
	LO <sub>1</sub>	-1.7	1.19	1.57

that modified by alloying depends on the slope  $\partial\omega/\partial x$ , and, furthermore, the calculated phonon dispersion of that branch is reconfirmed. Table I sums up the frequency shifts and the changes in the line asymmetry of the LO and TO lines upon ion bombardment, on which the discussion so far was based. In general the slope of the TO branch with alloying is more moderate than that of the LO branch, but this does not necessarily imply a similar effect on the asymmetry because of the different interactions involved. In the  $\text{Si}_x\text{Ge}_{1-x}$  alloy with no ionicity (triple degeneracy of the optic mode) the Raman lines are also asymmetric and the degree of the asymmetry is related to the respective bond gradients vs concentration.<sup>26</sup>

We therefore reach the conclusion that there is a fundamental difference in the kind of disorder induced by ion implantation and that caused by alloying. In the latter case the basic symmetry is maintained and therefore the Raman scattering takes place at  $k \sim 0$ . This calls for compliance with the selection rules in alloys, though not as strictly as in single crystals. In fact, as long as the excitation energy is significantly lower than the direct energy gap (1.96 eV compared with 2.41 eV), selection rules are generally obeyed and the  $z(xx)\bar{z}$  forbidden spectrum detected is of very low intensity as can be seen in Fig. 4(a). Yet, when the incident radiation is highly absorbed and in particular at resonance conditions, the forbidden LO lines in  $\text{Al}_{0.70}\text{Ga}_{0.30}\text{As}$  (as well as in other alloys) become rather intense and also several other lines emerge; this is demonstrated in Fig. 5. The appearance of resonant intense forbidden LO lines in alloys is explained in terms of the Fröhlich interaction of the elastically scattered excited electrons from the  $\Gamma$  valley of the conduction band towards the  $X$  valley and back via the random ion potential.<sup>27,28</sup> This explains why the removal of free carriers by the damage introduced via ion bombardment drastically reduces the forbidden LO lines (Fig. 5). Fig.

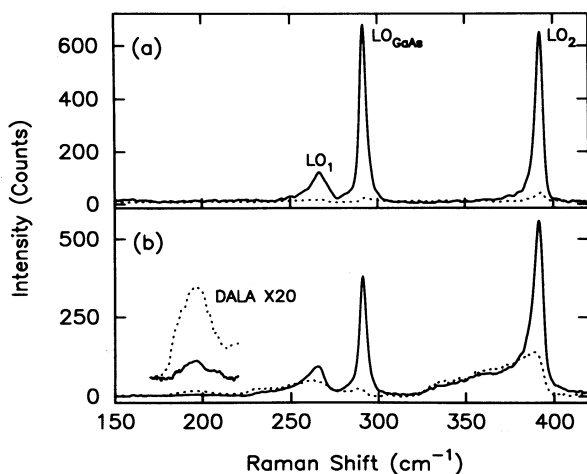


FIG. 4. Raman scattering excited at 1.96 eV in the  $z(yx)\bar{z}$  (solid line) and  $z(xx)\bar{z}$  (dotted line) configurations of  $\text{Al}_{0.70}\text{Ga}_{0.30}\text{As}$  pristine (a) and following ion implantation of  $1 \times 10^{14}$  ion cm<sup>-2</sup> (b) normalized to the same photon incident flux.  $\text{LO}_{\text{GaAs}}$  is the Raman scattering from the GaAs capping layer and the substrate, DALA is the disorder-activated longitudinal acoustic line.

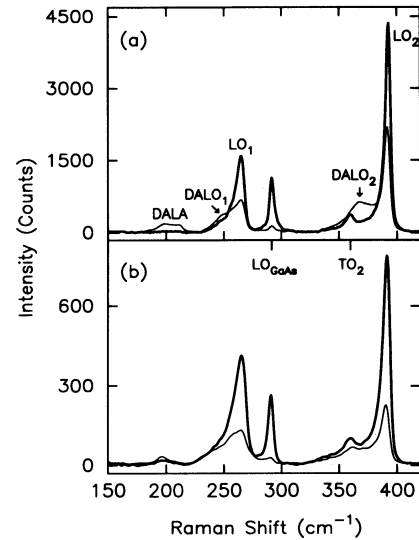


FIG. 5. The  $z(yx)\bar{z}$  (heavy line) and  $z(xx)\bar{z}$  (light line) Raman scattering excited at 2.41 eV from pristine  $\text{Al}_{0.70}\text{Ga}_{0.30}\text{As}$  (a) and following ion implantation of  $1 \times 10^{14}$  ion cm<sup>-2</sup> (b).  $\text{LO}_{\text{GaAs}}$  is the Raman scattering from the GaAs capping layer. DALA,  $\text{DALO}_1$ , and  $\text{DALO}_2$  are disorder-activated LA,  $\text{LO}_1$ , and  $\text{LO}_2$  lines, respectively.

ure 5 presents the Raman spectra, both allowed and forbidden, scattered from  $\text{Al}_{0.70}\text{Ga}_{0.30}\text{As}$  and comparison is made between a pristine section and an ion-bombarded section normalized to the same photon incident flux. Since the light penetration depth is reduced with the implantation and also the scattering intensity of the surviving crystallites is reduced, the intensity ratios of implanted to nonimplanted samples should be compared. This intensity ratio in the forbidden configuration is about half of that of the allowed one for ion bombardment of  $1 \times 10^{14}$  ion cm<sup>-2</sup> of  $\text{B}^+$  and almost vanishes at ion bombardment of  $1 \times 10^{15}$  ion cm<sup>-2</sup> of  $\text{B}^+$ .

As already mentioned, in addition to the forbidden LO lines,<sup>10</sup> other lines were observed in the  $z(xx)\bar{z}$  configuration [Fig. 5(a)] and were assigned as disorder-activated lines, DALA, DATO, DALO, etc.<sup>6,7,12,29,30</sup> These are found mainly in the indirect-gap compounds; in the present case we refer to  $\text{Al}_{0.70}\text{Ga}_{0.30}\text{As}$ . In a recent calculation, the intensity of these lines comes out lower than that of the allowed modes by two orders of magnitude.<sup>31</sup> Indeed, as shown in Fig. 4(a), for excitation energy below the direct electronic gap, these symmetry-forbidden lines diminish.<sup>32</sup> The DALA line, however, can be generated at off resonances by ion bombardment as shown in Fig. 4(b), which is not the case for the other disorder-activated lines. The DALA frequency range consists of two lines, at  $\sim 197$  and at  $\sim 210$  cm<sup>-1</sup>. These lines exhibit a different dependence on the excitation energy,<sup>30</sup> on concentration,<sup>31</sup> and also on ion implantation. Already at the modest dose of  $1 \times 10^{14}$  ion cm<sup>-2</sup> the 210-cm<sup>-1</sup> line disappears, while the 197-cm<sup>-1</sup> line is only slightly affected (Fig. 5). At higher doses a band reflecting the local phonon density of states appears and peaks around 197 cm<sup>-1</sup>. The LA zone-edge frequency is

independent of the Al content.<sup>14</sup>

The Raman line at  $\sim 368 \text{ cm}^{-1}$  is activated only near resonance. This line has a counterpart in the GaAs optic phonon range though of poorer resolution due to the relative dilution of the GaAs component. The  $368\text{-cm}^{-1}$  line was assigned as either DATO or DALO.<sup>7</sup> The DATO assignment is inconsistent with either the phonon-dispersion calculation<sup>14</sup> or with our results, which verify the negative slope of the TO branch. The assignment of this line as DALO<sub>2</sub> is tempting, because of its resemblance to LO<sub>2</sub> with respect to resonance enhancement and to frequency shift under high hydrostatic pressure (to be dealt with elsewhere). However, we claimed that the slope of the LO<sub>2</sub> dispersion is much smaller than that of LO<sub>1</sub> and also the calculated dispersion cannot support the DALO<sub>2</sub> assignment as such. The scenario we propose is as follows. The  $368\text{-cm}^{-1}$  line is indeed DALO<sub>2</sub>, which is activated solely by excited electrons being elastically scattered to the zone edge, where they have a significant kinetic energy. At that large  $k$  the correlation length is small, allowing for a high sensitivity to the selection of local sample compositions; therefore a smaller Al content is preferred. This line is rather broad and extends from LO<sub>2</sub> to TO<sub>2</sub>, but peaks at  $368 \text{ cm}^{-1}$ . We identify this peak with the DALO<sub>2</sub> line at an Al content of  $x \approx 0.4$ , at which the electronic energies at  $\Gamma$ ,  $X$ , and  $L$  cross. At lower Al content the energy gap is direct and this line disappears. This leaves us with a total AlAs LO dispersion of about  $12 \text{ cm}^{-1}$  (compared with  $49 \text{ cm}^{-1}$  of GaAs LO dispersion) and it also explains why, whenever the DALO<sub>2</sub> line appears, its frequency is insensitive to the composition. This was verified for Al<sub>0.85</sub>Ga<sub>0.15</sub>As. The DALO<sub>1</sub> line is also detected and its frequency distance from LO<sub>1</sub>( $\Gamma$ ) ( $\Delta\omega_1 = \omega[\text{LO}_1(\Gamma)] - \omega(\text{DALO}_1)$ ) is *smaller* than the respective one between the LO<sub>2</sub> and DALO<sub>2</sub> lines [Fig. 5(a)]; also the DALO<sub>1</sub> line was found to be insensitive to the composition. Two factors contribute to this result, namely, the decrease in  $\Delta\omega_1$ : (i)  $\Delta\omega_1$  becomes considerably smaller with the dilution of GaAs and (ii) the frequency of the DALO<sub>1</sub> line increases with the Ga content; thereby  $\omega(\text{DALO}_1)$  at  $x \approx 0.4$  causes  $\Delta\omega_1$  to shrink. We note that both DALO lines vanish with the implantation [Fig. 5(b)], giving rise to broad density-of-states-like structures, which peaks at the respective TO ranges.

For the sake of clarity, we have separated completely the mechanisms controlling the asymmetry caused by the ion-implantation damage and that caused by alloying. However, it should be understood that by doing that we meant to treat the dominant factor in each case, but it does not necessarily exclude the possibility that a decrease of the macroscopic electric field by the ion damage or a slight relaxation of the selection rules in alloys may thereby introduce some dependence on the phonon dispersion. Even in glasses the macroscopic field persists,<sup>33</sup> though it is slightly reduced. Also, the mixture with foreign atoms may modulate the electric field with a different frequency and thereby partially screen the mac-

roscopic electric field, causing the frequency to shift down towards the frequency of the TO mode. This means that the asymmetry is affected by the mode polarity and by the degree of screening of the electric field. Indeed, there is a high asymmetry in the more polar modes of alloys of both III-V and II-VI alloys.

We restricted our study to two-mode alloys, but it is interesting to extend this view of one-mode alloys as well. There are very few such systems and even those are suspected to have a semi-two-mode behavior.<sup>10</sup> A typical representative of this group of alloys is Ga<sub>*x*</sub>In<sub>1-*x*</sub>P. We refer here to the observation<sup>34</sup> that the lower-frequency mode, a TO mode, is asymmetrical and its symmetry changes sign with the concentration. It seems that this alloy is of two-mode type, and, since the two modes are quite close in frequency, the interaction between them is rather large and cannot be separated from the interaction within each individual mode (InP-like or GaP-like TO mode). A close examination shows that there is a noticeable change in the gradient of  $\omega(x)$ , which in spite of the complexity of the problem is generally speaking in line with the present approach. In interacting, but more defined two-mode alloys, the picture is clearer, as explained<sup>23</sup> in the case of Ga<sub>*x*</sub>In<sub>1-*x*</sub>As and as can be understood also in the system<sup>10</sup> of GaAs<sub>*x*</sub>Sb<sub>1-*x*</sub>. Though in these systems phonon-phonon interaction is far more complicated due to the proximity of the two oscillators, yet one can follow the arguments presented here to describe the behavior of the different phonons phenomenologically.

#### IV. CONCLUSIONS

In order to account for the modification of the phonon line shape and its frequency under ion bombardment, it is indeed necessary to make use of the phonon-dispersion relations along with the spatial-correlation model. By doing so one is also able to crudely probe the dispersion relation. On the other hand, it was shown that Raman scattering from phonons in two-mode alloys takes place at a small  $k$  and that the phonon line shapes are affected primarily by the slope of the frequency as a function of the fraction of the respective component. The ion bombardment of Al<sub>*x*</sub>Ga<sub>1-*x*</sub>As clearly distinguishes between the effect of crystallographic disorder and that of alloying via the response of the Raman lines. Assuming interaction between the various phonon modes having the same symmetry, oscillator strength is transferred from the less ionic (or weaker bonding) to the more ionic (or stronger bonding) mode, thereby producing line asymmetry as well as line broadening. In this framework, the disorder-activated modes were also treated and a mechanism for explaining their frequencies was proposed.

#### ACKNOWLEDGMENTS

This work was supported in part by the New York Metropolitan Research Fund and by the Fund for Promotion of Research at the Technion.

- <sup>1</sup>K. K. Tiong, P. M. Amirtharaj, F. H. Pollak, and D. E. Aspnes, *Appl. Phys. Lett.* **44**, 122 (1984).
- <sup>2</sup>R. S. Berg and P. Y. Yu, *Phys. Rev. B* **35**, 2205 (1987).
- <sup>3</sup>M. Holtz, R. Zallen, O. Brafman, and S. Matteson, *Phys. Rev. B* **37**, 4609 (1988).
- <sup>4</sup>D. R. Myers, P. L. Gourley, and P. S. Peercy, *J. Appl. Phys.* **54**, 5032 (1983).
- <sup>5</sup>P. Parayanthal and F. H. Pollak, *Phys. Rev. Lett.* **52**, 1822 (1984).
- <sup>6</sup>W. Xiao-jun and Z. Xin-yi, *Solid State Commun.* **59**, 869 (1986).
- <sup>7</sup>J. Leng, Y. Qian, P. Chen, and A. Madhukar, *Solid State Commun.* **69**, 311 (1989).
- <sup>8</sup>H. Richter, Z. P. Wang, and L. Ley, *Solid State Commun.* **39**, 625 (1981).
- <sup>9</sup>J. A. Kash, J. M. Hvam, J. C. Tsang, and T. F. Kuech, *Phys. Rev. B* **38**, 5776 (1988).
- <sup>10</sup>T. C. McGlinn, T. N. Krabach, M. V. Klein, G. Bajor, J. E. Greene, B. Kramer, S. A. Barnett, A. Lastras, and S. Gorbatskin, *Phys. Rev. B* **33**, 8396 (1986).
- <sup>11</sup>R. Zallen, *J. Non-Cryst. Solids* **141**, 227 (1992).
- <sup>12</sup>B. Jusserand and J. Sapriel, *Phys. Rev. B* **24**, 7194 (1981).
- <sup>13</sup>K. P. Jain and M. Balkanski, in *Proceedings of the Third International Conference on Light Scattering in Solids, Campinas, 1975*, edited by M. Balkanski, R. C. C. Leite, and S. P. S. Porto (Flammarion, Paris, 1976), p. 106.
- <sup>14</sup>S. Baroni, S. de Gironcoli, and P. Giannozzi, *Phys. Rev. Lett.* **65**, 84 (1990).
- <sup>15</sup>P. H. Borchers, G. F. Alfrey, D. H. Saunderson, and A. D. B. Woods, *J. Phys. C* **8**, 2022 (1975).
- <sup>16</sup>P. Giannozzi, S. de Gironcoli, P. Pavone, and S. Baroni, *Phys. Rev. B* **43**, 7231 (1991).
- <sup>17</sup>D. J. Mowbray, M. Cardona, and K. Ploog, *Phys. Rev. B* **43**, 1598 (1991).
- <sup>18</sup>G. Dolling and J. L. T. Waugh, in *Lattice Dynamics*, edited by R. F. Wallice (Pergamon, Oxford, 1965), p. 19.
- <sup>19</sup>C. A. Tran, J. L. Brebner, R. Leonelli, M. Jouanne, and R. A. Masut, *Phys. Rev. B* **49**, 11 268 (1994).
- <sup>20</sup>R. Borroff, R. Merlin, A. Chin, and P. K. Bhattacharya, *Appl. Phys. Lett.* **53**, 1652 (1988).
- <sup>21</sup>O. Brafman, I. F. Chang, G. Lengyel, S. S. Mitra, and E. Carnall, Jr., *Phys. Rev. Lett.* **19**, 1120 (1967).
- <sup>22</sup>G. P. Srivastava, J. L. Martins, and A. Zunger, *Phys. Rev. B* **31**, 2561 (1985).
- <sup>23</sup>G. Landa, H. Carles, and J. B. Renucci, *Solid State Commun.* **86**, 381 (1993).
- <sup>24</sup>H. W. Verleur and A. S. Barker, Jr., *Phys. Rev.* **149**, 715 (1966).
- <sup>25</sup>K. Shahzad, D. J. Olego, C. G. Van de Walle, and D. A. Cammack, *J. Lumin.* **46**, 109 (1990).
- <sup>26</sup>T. Ishidate, S. Katagiri, K. Inoue, M. Shibuya, T. Tsuji, and S. Minomura, *J. Phys. Soc. Jpn.* **53**, 2584 (1984).
- <sup>27</sup>M. E. Delaney, T. C. McGlinn, and M. V. Klein, *Phys. Rev. B* **44**, 8605 (1991).
- <sup>28</sup>R. M. Martin, *Phys. Rev. B* **10**, 2620 (1974).
- <sup>29</sup>R. Tsu, H. Kawamura, and L. Esaki, in *Proceedings of the Eleventh International Conference on the Physics of Semiconductors, Warsaw, 1972*, edited by M. Miasek (P. W. N. Polish-Scientific, Warsaw, 1972), p. 1135.
- <sup>30</sup>R. N. Carles, A. Saint-Criq, M. A. Renucci, and J. B. Renucci, *Nuovo Cimento D* **2**, 1712 (1983).
- <sup>31</sup>M. Bernasconi, L. Colombo, L. Miglio, and G. Benedek, *Phys. Rev. B* **43**, 14 447 (1991).
- <sup>32</sup>Tsu, Kawamura, and Esaki (Ref. 29) assigned the DALA line, which was shown for excitation energy well below the energy gap. In Fig. 4 we show that in  $\text{Al}_{0.70}\text{Ga}_{0.30}\text{As}$  excited by the same energy a line in the vicinity of the DALA line shows up only upon implantation.
- <sup>33</sup>F. L. Galeener, *Phys. Rev. B* **19**, 4292 (1979).
- <sup>34</sup>R. Beserman, C. Hirlimann, and M. Balkanski, *Solid State Commun.* **20**, 485 (1976).